JACS
JOURNAL OF THE AMERICAN CHEMICAL SOCIETY
Article
Cite This: J. Am. Chem. Soc. 2019, 141, 6609−6616
pubs.acs.org/JACS

Nonadditive Ion Effects Drive Both Collapse and Swelling of Thermoresponsive Polymers in Water

Ellen E. Bruce,[†,⊥] Pho T. Bui,[‡,⊥] Bradley A. Rogers,[‡] Paul S. Cremer,*[,‡,§] and Nico F. A. van der Vegt*[,†]

[†]Eduard-Zintl-Institut für Anorganische und Physikalische Chemie, Technische Universität Darmstadt, Alarich-Weiss-Straße 10, D-64287 Darmstadt, Germany

[‡]Department of Chemistry, The Pennsylvania State University, University Park, Pennsylvania 16802, United States

[§]Department of Biochemistry and Molecular Biology, The Pennsylvania State University, University Park, Pennsylvania 16802, United States

Supporting Information

ABSTRACT: When a mixture of two salts in an aqueous solution contains a weakly and a strongly hydrated anion, their combined effect is nonadditive. Herein, we report such nonadditive effects on the lower critical solution temperature (LCST) of poly(*N*-isopropylacrylamide) (PNiPAM) for a fixed concentration of Na_2SO_4 and an increasing concentration of NaI. Using molecular dynamics simulations and vibrational sum frequency spectroscopy, we demonstrate that at low concentrations of the weakly hydrated anion (I^-), the cations (Na^+) preferentially partition to the counterion cloud around the strongly hydrated anion (SO_4^{2-}), leaving I^- more hydrated. However, upon further increase in the NaI concentration, this weakly hydrated anion is forced out of solution to the polymer/water interface by sulfate. Thus, the LCST behavior of PNiPAM involves competing roles for ion hydration and polymer−iodide interactions. This concept can be generally applied to mixtures containing both a strongly and a weakly hydrated anion from the Hofmeister series.

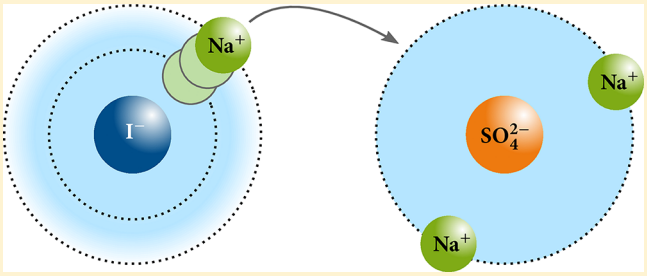

INTRODUCTION

Traditionally, the relative effects of anions on physical behavior in aqueous solutions have been ranked according to the Hofmeister series: $CO_3^{2-} > SO_4^{2-} > S_2O_3^{2-} > H_2PO_4^- > F^- > Cl^- > Br^- > NO_3^- > I^- > ClO_4^- > SCN^-$.[1,2] While weakly hydrated anions (right side of the series) partition to nonpolar environments such as air/water interfaces[3] or polymer surfaces,[4−6] strongly hydrated anions (left side of the series) prefer the bulk water environment. Herein, however, we demonstrate that the extent of hydration of a weakly hydrated anion can be modulated in the presence of a second strongly hydrated anion. As such, the current Hofmeister series needs to be updated to account for weakly hydrated anions' bifurcated behavior in mixed salt solutions.

The balance between an anion's affinity for water and for nonpolar environments can be exploited to regulate the phase behavior of polymers in aqueous solutions. The total effect of salts on polymer solubility is related to the behavior of both the anions and the cations, whose specific interactions are considered to be independent and additive. This idea goes back to the pioneering work of Guggenheim[7,8] and others[9−11] and is commonly used today to rationalize the actions of Hofmeister ions in chemistry and biology. Additionally, the assumption of additivity is consistent with the behavior of many single salts in the Hofmeister series.[12,13] Very recently, however, it has been argued that not only ion−macromolecule but also ion−counterion interactions in the bulk solution and at the interface can affect polymer phase transitions.[14,15] For example, deviations from the additivity assumption have been observed in systems containing guanidinium cations. These cations have varying abilities to form ion pairs at the macromolecule surface (cooperative binding) depending upon the counteranions with which they are paired.[16,17] This can lead to either polymer swelling or collapse.

Compared to single salts, fewer studies have focused on salt mixtures. Nonadditive effects on aqueous polymer solubility in mixed salt solutions have been reported for poly(propylene oxide) (thermodynamic measurements).[18] Additionally, it has been shown that strongly hydrated anions can drive weakly hydrated anions to the air/water interface in mixed electrolyte solutions (spectroscopic measurements and molecular dynamics (MD) simulations).[19] Although interesting effects from mixed salt solutions were observed in both of these works, the full range of the Hofmeister series has not yet been explored, and the molecular mechanisms remain elusive.

Herein, we report ion-specific effects on the lower critical solution temperature (LCST) of poly(*N*-isopropylacrylamide)

Received: January 9, 2019
Published: March 28, 2019

DOI: 10.1021/jacs.9b00295
J. Am. Chem. Soc. 2019, 141, 6609−6616

(PNiPAM) in three mixed salt solutions, namely NaI and Na_2SO_4, NaI and NaCl, as well as NaCl and Na_2SO_4. The most pronounced nonadditive features were observed for the combination of a weakly hydrated salt (i.e., NaI) and a strongly hydrated salt (i.e., Na_2SO_4). Significantly, it was found that ion hydration and polymer−anion interactions could be regulated in the presence of the weakly and strongly hydrated mixed salts, leading to both collapse and swelling transitions of the polymer. The underlying mechanisms are addressed using atomic-level insight obtained from MD simulations and vibrational sum frequency spectroscopy (VSFS).

Figure 1 schematically depicts the collapse and swelling behavior of PNiPAM in the presence of a fixed concentration

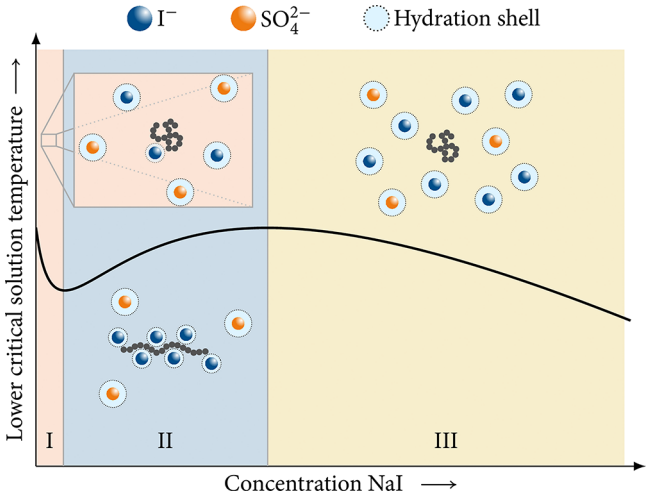

Figure 1. Schematic illustration of nonadditive ion effects on the lower critical solution temperature (LCST) of thermoresponsive polymers in aqueous solution containing a fixed concentration of a strongly hydrated salt (Na_2SO_4) and an increasing concentration of a weakly hydrated salt (NaI). In region I, enhanced iodide hydration drives polymer collapse. In region II, SO_4^{2-} salts out I^-, which in turn becomes enriched at the polymer/water interface, driving polymer swelling. In region III, enhanced ion hydration again drives polymer collapse.

of Na_2SO_4 and an increasing concentration of NaI. The nonadditive effects were observed at low concentration (region I) and intermediate concentration (region II) of NaI. At low NaI concentration (region I), the presence of Na_2SO_4 does not significantly affect the interaction between iodide and the polymer. Counterintuitively, the polymer collapses more readily. The VSFS measurements and MD simulations suggest that sodium cations preferentially partition to the counterion cloud around sulfate, resulting in a lower excess counterion density around iodide. As such, iodide becomes more hydrated and drives polymer collapse.[20] This effect is saturable, and upon further addition of NaI, a re-entrant behavior of the polymer is observed in region II. Under these conditions, the strongly hydrated salt (Na_2SO_4) affects the solubility of the weakly hydrated salt (NaI), in accordance with the mechanism proposed in an earlier work.[19] Specifically, more iodide adsorbs to the polymer, leading to swelling. When the NaI concentration is increased even further (region III), the polymer again collapses, driven by the depletion of hydrated ions. The nonadditive ion effects observed herein shed new light on Hofmeister ion chemistry and should help provide new insights into a broad range of complex mixed electrolyte solutions such as ocean waters, dense cellular environments, and multicomponent ion solutions found in a typical chemistry laboratory.[21−23]

RESULTS AND DISCUSSION

Lower Critical Solution Temperature of PNiPAM in Aqueous Salt Solutions. PNiPAM displays an inverse phase transition above its LCST. Herein, we systematically investigated the change in the LCST of PNiPAM in the presence of fixed concentrations of Na_2SO_4 and increasing concentration of NaI. The LCST was determined from the turbidity changes of polymer solutions as a function of temperature. More details on the LCST measurements can be found in the Supporting Information. As shown in Figure 2a, in the absence of Na_2SO_4, the LCST of PNiPAM initially increases, reaches a maximum, and then decreases upon adding NaI (dark blue curve), consistent with earlier observations.[4] Interestingly, in mixed salt solutions, the solubility of PNiPAM depends on the concentration of NaI, the type of added salt

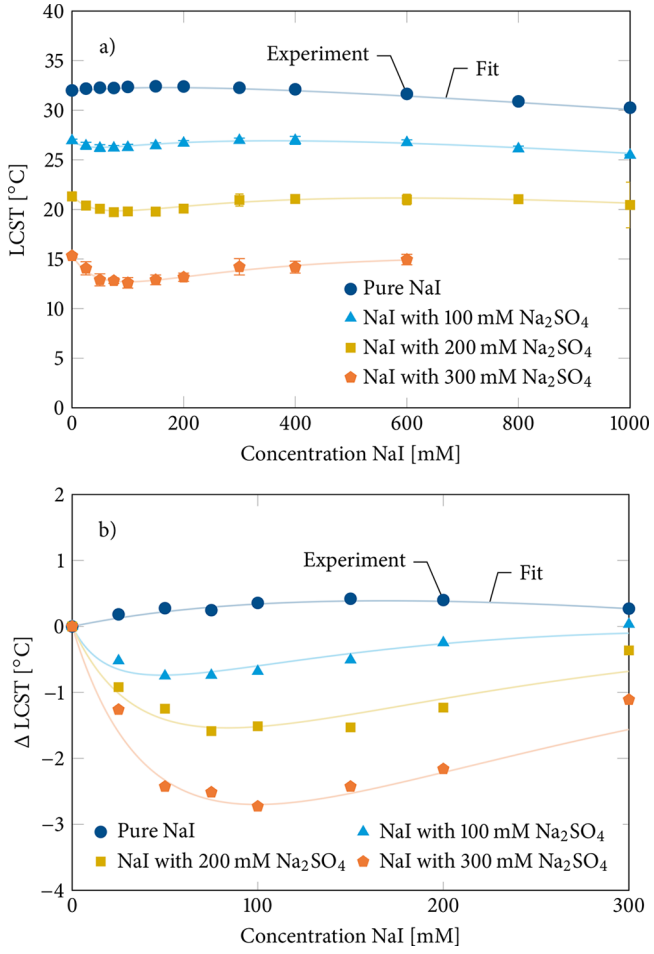

Figure 2. (a) Lower critical solution temperature (LCST) and (b) the change in LCST (ΔLCST) of PNiPAM upon the addition of NaI with 0 mM, 100 mM, 200 mM, and 300 mM Na_2SO_4 as the background salt. Note that ΔLCST is only shown for data points within the 0−300 mM NaI concentration range in order to highlight the dip in the LCST. The error bars are calculated from sample standard deviations from three sets of measurements. See Figure S1 for the error bars corresponding to the ΔLCST values. The fits correspond to the empirical model given in eq 1. The fitting parameters are reported in Table 1.

DOI: 10.1021/jacs.9b00295
J. Am. Chem. Soc. 2019, 141, 6609−6616

(the background salt), as well as its concentration. In the presence of the highest Na_2SO_4 background concentration (orange curve), the LCST behavior can be divided into three NaI concentration regions: region I (0−100 mM), region II (100−600 mM), and region III (>600 mM). At lower Na_2SO_4 concentrations, the boundary between regions II and III shifts to lower NaI concentration. In the presence of Na_2SO_4, the LCST decreases in region I, in marked contrast to the increase observed in the pure NaI system. Upon further addition of NaI, the LCST increases (region II) and then eventually decreases (region III) in the presence of 100 mM and 200 mM Na_2SO_4 (light blue and yellow curves, respectively). With 300 mM Na_2SO_4, this decrease is not observed (orange curve) but would presumably occur at a higher NaI concentration, if the solubility limit of the salts was not reached. The magnitude of the initial decrease, which is manifested as a dip, is dependent on the background salt concentration. For comparison, ΔLCST, defined as the change in the LCST upon adding NaI, is shown in Figure 2b. The dip becomes more pronounced as the concentration of the background salt increases.

The LCST of PNiPAM as a function of NaI concentration can be empirically modeled by

$$T = T_0 + ac_{salt} + \frac{B_{max,1}c_{salt}}{K_{D,1} + c_{salt}} + \frac{B_{max,2}c_{salt}}{K_{D,2} + c_{salt}} \quad (1)$$

where T_0 is the LCST in the absence of NaI, and ac_{salt} (with c_{salt} being the NaI concentration) is a linear term related to the surface tension at the polymer/water interface. The third term is a Langmuir binding isotherm, which quantifies the magnitude of the increase in the LCST from the initial LCST (T_0) due to iodide adsorption to the PNiPAM chain. The dissociation constant ($K_{D,1}$) quantifies the strength of the iodide adsorption process, which at saturation produces a maximum increase in the LCST ($B_{max,1}$). The LCST of PNiPAM in single electrolyte solutions can be fully explained by the first three terms and has been utilized previously.[4] The fourth term, which is needed to describe mixed salt solutions, is reminiscent of a Langmuir binding isotherm but originates from ion pairing and ion hydration. This term quantifies the decrease in the LCST due to enhanced iodide hydration and has a negative $B_{max,2}$ value. The fitting parameters are summarized in Table 1. More details on the fitting procedure are provided in the Supporting Information.

Table 1. Fitting Parameters (T_0, a, $B_{max,1}$, $K_{D,1}$, $B_{max,2}$, and $K_{D,2}$) for the Empirical Lower Critical Solution Temperature Model of PNiPAM in NaI and Mixtures of NaI with Na_2SO_4 Given by Equation 1[a]

	Na_2SO_4 concentration [mM]			
	0	100	200	300
T_0 [°C]	31.9	27.0	21.4	15.4
a [°C/mM]	← -4.2×10^{-3} →			
$B_{max,1}$ [°C]	3.1	6.9	14.9	23.8
$K_{D,1}$ [mM]	← 308.1 →			
$B_{max,2}$ [°C]	–	−2.5	−8.6	−15.9
$K_{D,2}$ [mM]	–	33.8	81.0	96.0

[a]The parameters a and $K_{D,1}$ are independent of the Na_2SO_4 concentration (see Supporting Information).

Polymer−Ion Interactions. To elucidate the mechanisms of nonadditivity in the LCST measurements, we analyzed the number of iodide ions in proximity to a PNiPAM 5-mer (oligomer) using MD simulations. Details concerning the simulations and the force fields can be found in the Methods section and in Table S1 in the Supporting Information, respectively. Note that while molarity is used to describe concentration in the experiments, molality is used in the simulations where 0.1 m is equivalent to 100 mM. The difference between the two units is negligible within the range considered in these studies. Figure 3 shows the number of iodide ions in proximity to the oligomer surface as defined by the first peak of the proximal radial distribution function.

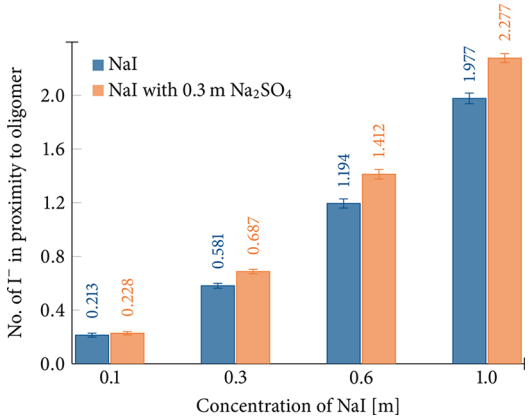

Figure 3. Number of iodide ions in proximity to the PNiPAM oligomer at different concentrations of NaI in the absence (blue bars) and presence (orange bars) of 0.3 m Na_2SO_4. The proximity is defined by the first peak in the proximal radial distribution function between the oligomer surface and iodide and is equal to 0.52 nm. The error bars are error estimates calculated from 20 blocks and sample standard deviations.

In region I (0.1 m NaI), the number of iodide ions is not affected by the presence of Na_2SO_4, yet the polymer collapses more readily. By contrast, in regions II and III, Na_2SO_4 pushes iodide toward the PNiPAM/water interface. This agrees with the observed increase in $B_{max,1}$ as Na_2SO_4 concentration increases (Table 1). In a mixed electrolyte solution, the strongly hydrated salt may salt out the weakly hydrated salt, as has previously been demonstrated by monitoring ions at the air/water interface with a combination of photoelectron spectroscopy and MD simulations.[19] Our simulations confirm that the surface enhancement of the large polarizable anion (I^-) is driven by the strongly hydrated ion (SO_4^{2-}). As such, the observed increase in the LCST in region II results from a forced iodide adsorption effect.

The iodide−polymer interactions were further explored using VSFS measurements. To do this, a Gibbs monolayer of PNiPAM was formed at the air/water interface in the presence of salts in the subphase, as schematically shown in Figure 4a. More details on the VSFS measurements are described in the Supporting Information. Figure 4b shows the OH stretch region (3000−3800 cm^{-1}) of the air/PNiPAM/water interface in pure Na_2SO_4 and mixtures of Na_2SO_4 and NaI. For complete spectra (2800−3800 cm^{-1}) as a function of NaI concentration in the absence and presence of Na_2SO_4, see Figure S2. The peak assignments and the fitting parameters are summarized in Table S2 and Table S3. The spectra are

DOI: 10.1021/jacs.9b00295
J. Am. Chem. Soc. 2019, 141, 6609−6616

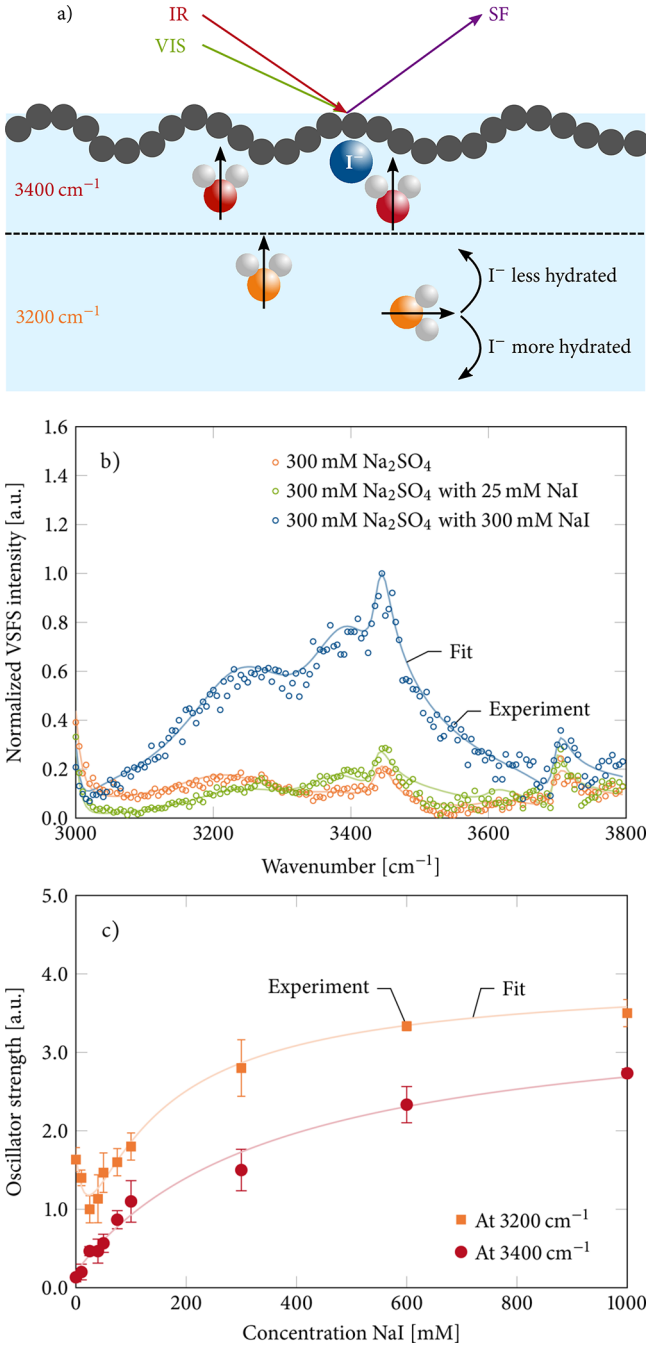

Figure 4. (a) Schematic illustration of the orientation of the water molecules at the air/PNiPAM/water interface in the absence and presence of salts. Two major water populations are colored in red (3400 cm^{-1}) and orange (3200 cm^{-1}), with the black arrows indicating the direction of the water dipoles. The curved arrows indicate possible disruptions of the alignment. (b) Vibrational sum frequency spectroscopy (VSFS) spectra of the water region (3000–3800 cm^{-1}) of a PNiPAM monolayer at the air/water interface in the presence of 300 mM Na_2SO_4 background and 0 mM (orange), 25 mM (green), and 300 mM (blue) NaI in the subphase. The data were fitted using eq S2. See Table S3 for peak assignments and fitting parameters. (c) The oscillator strengths at 3200 cm^{-1} (orange) and 3400 cm^{-1} (red) as a function of the NaI concentration in the presence of 300 mM Na_2SO_4. The error bars are calculated from standard deviations from three sets of measurements. Equation S3 was used to fit the data, and Table S4 provides the fitting parameters.

dominated by two broad features at 3200 and 3400 cm^{-1}, consistent with previous studies of this interface.[24] The 3200 cm^{-1} peak reports on more ordered water molecules, while the peak around 3400 cm^{-1} arises from water molecules with less ordered hydrogen bonds.[25−27] It has been previously shown that this lower coordination water population (3400 cm^{-1}) is closer to the interface because that is where registry between interfacial water molecules and hydrogen bond donors/acceptors from adjacent organic or inorganic layers is most easily disrupted (red water molecules, Figure 4a).[28] Further away from the interface, it is possible to achieve more tetrahedral water structure, giving rise to the peak around 3200 cm^{-1} (orange water molecules).[28] As such, the 3200 cm^{-1} feature should represent water molecules that are further away from the polymer surface and are aligned by the interfacial potential, while the 3400 cm^{-1} feature should arise mostly from the water structure in the inner hydration shell of the polymer, adjacent to the polymer/water interface.

Upon introducing NaI to the subphase, the oscillator strength of the 3400 cm^{-1} peak increases monotonically (red curve in Figure 4c). This increase is consistent with the direct adsorption of I$^-$ to the PNiPAM surface, which aligns water molecules in the first hydration layer (red water molecules, Figure 4a). At higher NaI concentration, the surface becomes saturated with iodide, and the oscillator strength of the 3400 cm^{-1} peak approaches a maximum value, $B_{max,1}$ (Table S4). The value of $B_{max,1}$ in the presence of Na_2SO_4 is larger than that in the pure NaI case (Table S4), supporting the notion of enhanced iodide loading found in the MD simulations (Figure 3).

By contrast with the 3400 cm^{-1} peak, the oscillator strength of the 3200 cm^{-1} resonance decreases and then increases as NaI is added to the solution (orange curve in Figure 4c). The dip in the oscillator strength is reminiscent of the dip in the LCST measurements. Presumably, the minimum occurs at a lower NaI concentration in the VSFS experiments because of differences in the binding sites exposed to water for polymers in the bulk solution (LCST measurements) versus at the Gibbs monolayer (VSFS measurements). In pure NaI solutions, a monotonic increase in the oscillator strength of the 3200 cm^{-1} peak is observed and is related to the change in the interfacial potential as iodide binds to the surface (light blue curve in Figure S2c). By contrast, in pure Na_2SO_4 solutions, the oscillator strength of the 3200 cm^{-1} peak continuously decreases (Figure S3). This decreasing trend is caused by disruption in the alignment of water molecules further from the polymer surface as more well-hydrated ions are introduced. As such, the initial decrease in the oscillator strength of the 3200 cm^{-1} peak in the mixtures of NaI with Na_2SO_4 implies that iodide behaves like a strongly hydrated ion in region I of mixed salt solutions.

Ion Pairing and Ion Hydration. The nonmonotonic response of the 3200 cm^{-1} peak in the salt mixture suggests that the behavior of iodide beyond the first hydration shell of PNiPAM is distinct from that in the pure NaI solution. MD simulations were performed on bulk solutions, i.e., without PNiPAM, to explore the nature of ion pairing and ion hydration in single and mixed salt solutions. The ion pairing affinity between an anion and a cation (ΔN), also referred to as the excess ion pairing, is defined as

$$\Delta N = \frac{N_{cat}}{V}\int_0^{r_2}[g_{an,cat}(r) - 1]4\pi r^2 dr \quad (2)$$

DOI: 10.1021/jacs.9b00295
J. Am. Chem. Soc. 2019, 141, 6609−6616

where $g_{an,cat}(r)$ is the anion−cation radial distribution function, and N_{cat}/V is the number density of cations, here sodium ions. ΔN is determined by the balance of ion−ion, ion−water, and water−water (hydrogen bonding) interactions and can be interpreted as the change in the number of cations in a spherical observation volume of radius r_2 before and after placing an anion at the center of that region. r_2 is picked to include both contact ion pairs (CIPs) and solvent-shared ion pairs (SIPs).[29] As can be seen in Figure 5a, excess ion pairing between iodide and sodium decreases in the presence of Na_2SO_4 (orange data points) compared to in pure NaI solutions (blue data points). In contrast, Figure 5b shows that the excess ion pairing between sulfate and sodium increases as NaI is added to Na_2SO_4. Significantly, some sodium ions from the introduction of the NaI partition from iodide to the counterion cloud around sulfate in the mixed salt case.

This partitioning of sodium cations has a profound effect on iodide hydration. The anion−water affinity (ΔN) was quantified using an equation similar to eq 2 (see eq S5 for definition) where the anion−cation terms are replaced by anion−water equivalents and r_2 is the radius of the second hydration shell. The water affinity of iodide increases (orange data points in Figure 5c) in mixed salt systems compared to the pure NaI systems (blue data points). Iodide ions therefore become more hydrated in the presence of Na_2SO_4. Detailed analysis of the MD simulations including the CIPs and SIPs as well as the first and second hydration shells for the anions in various mixtures are summarized in Figures S4−9. Similar trends for ion pairing and ion hydration were observed in the simulations at various temperatures (Figure S10), suggesting that this mechanism is operative across the temperature range spanned by the LCST measurements.

Mechanisms of Nonadditivity in Mixed Salt Solutions. The LCST of PNiPAM displays pronounced signatures of nonadditivity upon the addition of NaI to solutions containing a fixed concentration of Na_2SO_4 (Figure 2). The combination of VSFS measurements and MD simulations reveals that SO_4^{2-} enhances the iodide−water affinity in the bulk solution, while simultaneously driving I^- to the polymer/water interface. These two effects provide a molecular-level mechanism for the observed nonadditivity in salt mixtures containing weakly and strongly hydrated anions with a common cation. A schematic illustration of this mechanism is provided in Figure 6. The concentration dependence of these two effects is distinct and gives rise to the three regions in the LCST phase diagram. At low concentrations of NaI (region I), Na^+ is recruited into the counterion cloud of SO_4^{2-} (black curved arrow in Figure 6), leaving I^- more hydrated than in a pure salt solution. The enhanced iodide−water affinity in the presence of SO_4^{2-} increases the NaI activity[29,30] and drives the salting out effect observed in region I. At intermediate NaI concentrations (region II), I^- is forced out of solution to the polymer/water interface by SO_4^{2-}. The enhanced binding of I^- to the polymer dominates over the enhanced hydration effect and gives rise to reentrant swelling of the PNiPAM chain. At the highest concentrations of NaI (region III), the addition of more salt decreases the LCST in a manner similar to the single salt case. This effect is related to the increased surface tension at the polymer/water interface.

Other Mixed Salt Cases. Using NaCl in place of Na_2SO_4 as the background salt, we demonstrate that the valency of the background anion, rather than its identity, is crucial for the nonadditive behavior of mixed salt solutions.[31,32] In the presence of NaCl, adding NaI produced a smaller dip in the LCST (Figure S11 and Table S5). This is expected, as the countercation cloud around a divalent ion (i.e., SO_4^{2-}) is

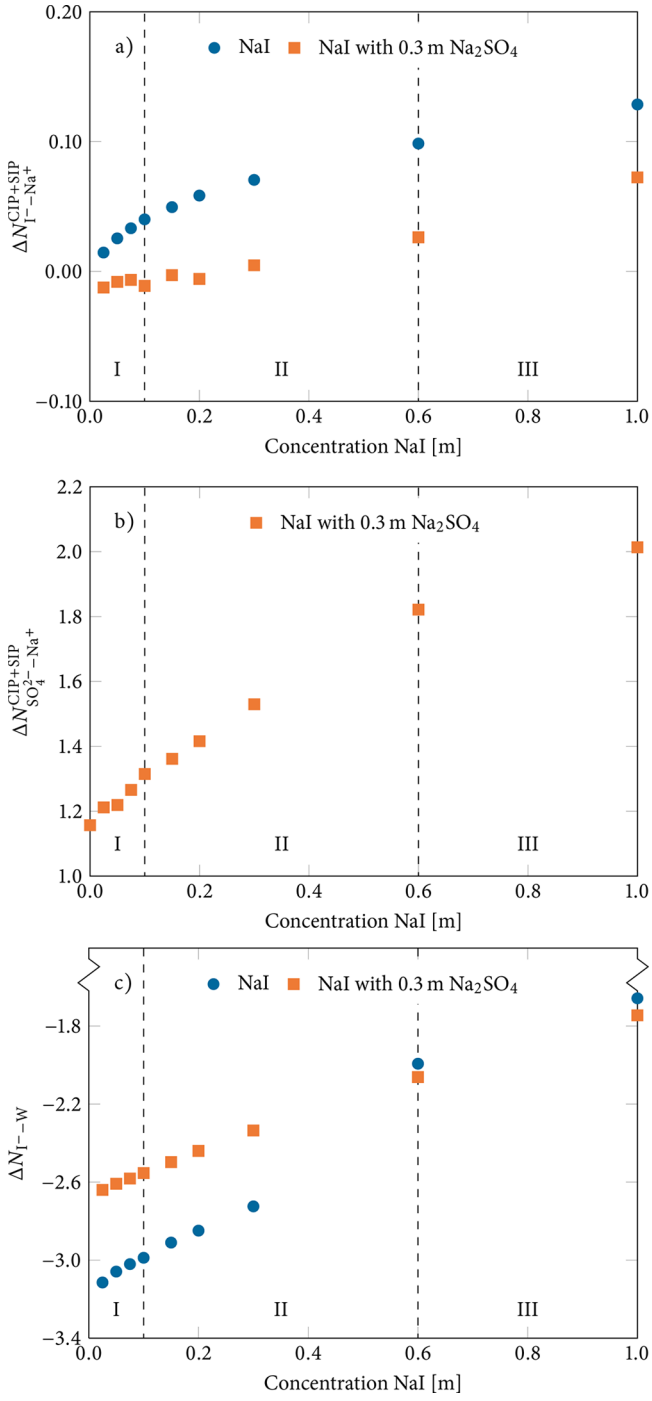

Figure 5. (a) Excess ion pairing between iodide and sodium for both contact and solvent-shared ion pairs (CIP+SIP) as a function of NaI concentration in the absence (blue) and presence (orange) of 0.3 m Na_2SO_4. (b) Excess ion pairing between sulfate and sodium for both contact and solvent-shared ion pairs (CIP+SIP) as a function of NaI concentration in the presence of 0.3 m Na_2SO_4. (c) Iodide−water affinity as a function of NaI concentration in the absence (blue) and presence (orange) of 0.3 m Na_2SO_4. The dashed lines show the boundaries between regions I, II, and III. The error bars are error estimates calculated from 20 blocks and sample standard deviations and are smaller than the symbols.

DOI: 10.1021/jacs.9b00295
J. Am. Chem. Soc. 2019, 141, 6609−6616

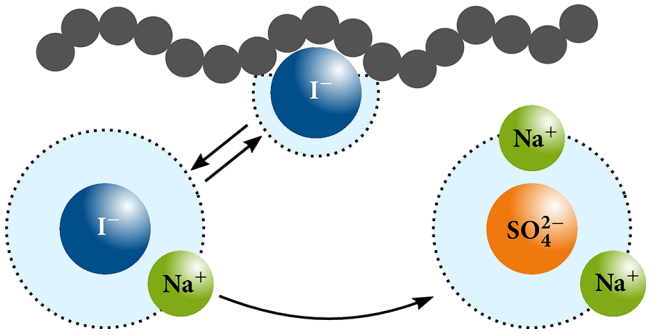

Figure 6. Schematic illustration of the mechanisms of nonadditivity in mixed salt solutions. The chain of gray spheres represents the polymer, while the anion hydration shells are drawn as black dashed circles. The partitioning of Na^+ from I^- to SO_4^{2-}, depicted by the curved arrow, causes I^- to be more hydrated and thereby drives polymer collapse. The adsorption of I^- to the polymer/water interface, influenced by Na_2SO_4, affecting the solubility of iodide drives polymer swelling instead. The flexible hydration shell of iodide causing the bifurcated behavior is indicated by the double arrows.

denser than the one around a monovalent ion (i.e., Cl^-). This idea concurs with the known pairing affinity between Na^+ and anions in pure salt solutions, which follows the series SO_4^{2-} > Cl^- > I^- with dissociation constants of 150 mM,[33] 250 mM,[34] and 1.4 M,[35] respectively. That is, the partitioning of Na^+ from the countercation cloud around I^- to the one around Cl^- is less effective than to the one around SO_4^{2-}, leaving iodide less hydrated in the former case. As such, the nonadditive effect in mixtures containing a divalent and a monovalent anion is substantially more pronounced than when both anions are monovalent. Moreover, further increase in the NaI concentration only causes a subtle increase in the LCST of PNiPAM in region II, followed by a decrease in region III (Figure S11). As a background anion, Cl^- is simply not as strongly hydrated as SO_4^{2-}. Therefore, it cannot salt iodide out of solution very effectively. This results in a smaller driving force for iodide to adsorb to the polymer/water interface, as reflected in the number of iodide ions in proximity with a PNiPAM 5-mer in MD simulations (Figure S12) and a smaller $B_{max,1}$ value for chloride than for sulfate (Table S5). Finally, region III looks mostly the same when NaCl replaces Na_2SO_4.

Next, in order to test whether the flexibility of an anion's hydration shell is essential for displaying nonadditive behavior, we also ran experiments where NaI was switched for NaCl in the presence of Na_2SO_4 as the background salt. Interestingly, no evidence was found for nonadditivity in regions I and II (Figure S13 and Table S6). The excess ion pairing between chloride and sodium increases in the presence of Na_2SO_4 (Figure S5), in contrast to the decreasing excess ion pairing between iodide and sodium. Similar to NaI, the presence of NaCl causes an increase in the pairing affinity between sulfate and sodium ions (Figure S6). However, the pairing affinity is less pronounced than in the presence of NaI, originating from sodium pairing more strongly with chloride than with iodide. Thus, a negligible preferential partitioning of sodium ions from the counterion cloud around chloride to that around sulfate is observed. Consequentially, the hydration shell around chloride is less affected than the one around iodide in the presence of Na_2SO_4 (Figure S8 and Figure S7). In fact, this observation is consistent with previous studies, which showed that the increase in ion pairing affinity between SO_4^{2-} and Na^+ is smaller in the presence of NaCl[36] than in the presence of $NaClO_4$,[37] another weakly hydrated anion. Compared to the mixture containing NaI and Na_2SO_4, the less flexible hydration shell for chloride leads to a shallower decrease in the LCST in region I in the presence of Na_2SO_4. Additionally, both chloride and sulfate remain well-hydrated and thus salt out the polymer at all concentrations of NaCl (Figure S13).

Using Different Polymers. Other thermoresponsive polymers were investigated with mixed salts in addition to PNiPAM. A dip feature in the LCST could also be observed with poly(*N*,*N*-dimethylacrylamide) (PDMA) in mixtures of NaI and Na_2SO_4 (Figure S14a) as well as with polyethylene glycol (PEG) in mixtures of NaSCN with Na_3PO_4 (Figure S14b). The fitting parameters are provided in Table S7. As such, the LCST behavior observed herein for PNiPAM with NaI and Na_2SO_4 is quite generic. Interestingly, the magnitudes and positions of the dip clearly depend on polymer chemistry as well as on the ion identities. Such differences are expected since the driving forces for nonadditivity of mixed salt solutions come from a competition between ion hydration in the bulk solution (universal behavior) and polymer−anion interactions, whereby the latter should be polymer specific.

CONCLUSIONS

We have shown that the phase behavior of PNiPAM in aqueous mixed salt solutions is determined by the subtle balance of ion hydration and direct interactions of weakly hydrated anions with the polymer. Significantly, in the presence of the strongly hydrated anion (i.e., SO_4^{2-}), the weakly hydrated anion (i.e., I^-) exhibits bifurcated behavior, driving consecutive polymer collapse and swelling transitions. In mixed salt solutions, sodium cations preferentially partition to the counterion cloud around sulfate, leaving iodide more hydrated in the bulk solution, driving polymer collapse. Concurrently, the strongly hydrated anion salts out the weakly hydrated anion to the polymer surface, causing polymer swelling.

The work reported herein illustrates that nonadditive ion effects in mixed salt solutions are caused by changes in the water affinity of weakly hydrated anions. The flexible hydration shell behavior, demonstrated with I^- in this work, is expected to apply to other weakly hydrated anions, such as SCN^- and ClO_4^-. We expect that these new insights into Hofmeister ion chemistry will have consequences beyond the newly discovered effects on the aqueous polymer solubility reported herein. This is quite significant, as the origins of the Hofmeister series in single salt solutions are just now beginning to be understood. Significantly more work will need to be done to understand the behavior of complex environments, like the solutions inside living cells, the brine solutions of ocean waters, as well as the numerous solutions employed in electrochemical setups, where a large number of different ions can be present simultaneously.

ASSOCIATED CONTENT

Supporting Information

The Supporting Information is available free of charge on the ACS Publications website at DOI: 10.1021/jacs.9b00295.

Methods, validation of sodium sulfate force field, additional experimental data, additional simulation data, lower critical solution temperature fitting, and vibrational sum frequency spectroscopy fitting (PDF)

DOI: 10.1021/jacs.9b00295
J. Am. Chem. Soc. 2019, 141, 6609−6616

AUTHOR INFORMATION

Corresponding Authors

*psc11@psu.edu

*vandervegt@cpc.tu-darmstadt.de

ORCID

Paul S. Cremer: 0000-0002-8524-0438

Nico F. A. van der Vegt: 0000-0003-2880-6383

Author Contributions

⊥E.E.B. and P.T.B. contributed equally to this work

Notes

The authors declare no competing financial interest.

ACKNOWLEDGMENTS

The simulations for this research were conducted on the Lichtenberg high performance computer at the TU Darmstadt. Furthermore, the Darmstadt authors thank the LOEWE project from iNAPO which is funded by the Ministry for Higher Education, Research and the Arts (HMWK) of the state of Hessen. The Penn State authors thank the National Science Foundation (CHE-1709735) for support. Additionally, the authors thank William Hunn, Kelvin Rembert, and Halil Okur for the initial observation of the nonadditive ion effects on lower critical solution temperature (LCST) measurements and Dr. Tinglu Yang for maintenance of the vibrational sum frequency spectroscopy system.

REFERENCES

(1) Hofmeister, F. Zur Lehre von der Wirkung der Salze. *Archiv f. experiment. Pathol. u. Pharmakol.* **1888**, *25*, 1−30.

(2) Kunz, W.; Henle, J.; Ninham, B. W. 'Zur Lehre von der Wirkung der Salze' (About the Science of the Effect of Salts): Franz Hofmeister's Historical Papers. *Curr. Opin. Colloid Interface Sci.* **2004**, *9*, 19−37.

(3) Jungwirth, P.; Tobias, D. J. Molecular Structure of Salt Solutions: A New View of the Interface with Implications for Heterogeneous Atmospheric Chemistry. *J. Phys. Chem. B* **2001**, *105*, 10468−10472.

(4) Zhang, Y.; Furyk, S.; Bergbreiter, D. E.; Cremer, P. S. Specific Ion Effects on the Water Solubility of Macromolecules: PNIPAM and the Hofmeister Series. *J. Am. Chem. Soc.* **2005**, *127*, 14505−14510.

(5) Cho, Y.; Zhang, Y.; Christensen, T.; Sagle, L. B.; Chilkoti, A.; Cremer, P. S. Effects of Hofmeister Anions on the Phase Transition Temperature of Elastin-Like Polypeptides. *J. Phys. Chem. B* **2008**, *112*, 13765−13771.

(6) Rembert, K. B.; Okur, H. I.; Hilty, C.; Cremer, P. S. An NH Moiety is Not Required for Anion Binding to Amides in Aqueous Solution. *Langmuir* **2015**, *31*, 3459−3464.

(7) Guggenheim, E. A. The Specific Thermodynamic Properties of Aqueous Solutions of Strong Electrolytes. *London, Edinburgh, Dublin Philos. Mag. J. Sci.* **1935**, *19*, 588−643.

(8) Guggenheim, E. A.; Turgeon, J. C. Specific Interaction of Ions. *Trans. Faraday Soc.* **1955**, *51*, 747−761.

(9) Brönsted, J. N. Studies on Solubility. IV. The Principle of the Specific Interactions of Ions. *J. Am. Chem. Soc.* **1922**, *44*, 877−898.

(10) Brönsted, J. N. The Individual Thermodynamic Properties of Ions. *J. Am. Chem. Soc.* **1923**, *45*, 2898−2910.

(11) Collins, K. D.; Washabaugh, M. W. The Hofmeister Effect and the Behaviour of Water at Interfaces. *Q. Rev. Biophys.* **1985**, *18*, 323−422.

(12) Pegram, L. M.; Record, M. T. Hofmeister Salt Effects on Surface Tension Arise from Partitioning of Anions and Cations Between Bulk Water and the Air−Water Interface. *J. Phys. Chem. B* **2007**, *111*, 5411−5417.

(13) Pegram, L. M.; Record, M. T. Thermodynamic Origin of Hofmeister Ion Effects. *J. Phys. Chem. B* **2008**, *112*, 9428−9436.

(14) Schneider, C. P.; Shukla, D.; Trout, B. L. Arginine and the Hofmeister Series: The Role of Ion−Ion Interactions in Protein Aggregation Suppression. *J. Phys. Chem. B* **2011**, *115*, 7447−7458.

(15) Jungwirth, P.; Cremer, P. S. Beyond Hofmeister. *Nat. Chem.* **2014**, *6*, 261−263.

(16) Heyda, J.; Okur, H. I.; Hladílková, J.; Rembert, K. B.; Hunn, W.; Yang, T.; Dzubiella, J.; Jungwirth, P.; Cremer, P. S. Guanidinium can Both Cause and Prevent the Hydrophobic Collapse of Biomacromolecules. *J. Am. Chem. Soc.* **2017**, *139*, 863−870.

(17) Balos, V.; Bonn, M.; Hunger, J. Anionic and Cationic Hofmeister Effects are Non-Additive for Guanidinium Salts. *Phys. Chem. Chem. Phys.* **2017**, *19*, 9724−9728.

(18) Moghaddam, S. Z.; Thormann, E. Hofmeister Effect of Salt Mixtures on Thermo-Responsive Poly(propylene oxide). *Phys. Chem. Chem. Phys.* **2015**, *17*, 6359−6366.

(19) Ottosson, N.; Heyda, J.; Wernersson, E.; Pokapanich, W.; Svensson, S.; Winter, B.; Öhrwall, G.; Jungwirth, P.; Björneholm, O. The Influence of Concentration on the Molecular Surface Structure of Simple and Mixed Aqueous Electrolytes. *Phys. Chem. Chem. Phys.* **2010**, *12*, 10693−10700.

(20) van der Vegt, N. F. A.; Nayar, D. The Hydrophobic Effect and the Role of Cosolvents. *J. Phys. Chem. B* **2017**, *121*, 9986−9998.

(21) Morris, A. W.; Riley, J. P. The Bromide/Chlorinity and Sulphate/Chlorinity Ratio in Sea Water. *Deep-Sea Res. Oceanogr. Abstr.* **1966**, *13*, 699−705.

(22) Lo Nostro, P.; Ninham, B. W. Hofmeister Phenomena: An Update on Ion Specificity in Biology. *Chem. Rev.* **2012**, *112*, 2286−2322.

(23) Vo, B. S.; Shallcross, D. C. Modeling Solution Phase Behavior in Multicomponent Ion Exchange Equilibria Involving H+, Na+, K+, Mg2+, and Ca2+ Ions. *J. Chem. Eng. Data* **2005**, *50*, 1995−2002.

(24) Chen, X.; Yang, T.; Kataoka, S.; Cremer, P. S. Specific Ion Effects on Interfacial Water Structure near Macromolecules. *J. Am. Chem. Soc.* **2007**, *129*, 12272−12279.

(25) Du, Q.; Freysz, E.; Shen, Y. R. Vibrational Spectra of Water Molecules at Quartz/Water Interfaces. *Phys. Rev. Lett.* **1994**, *72*, 238−241.

(26) Richmond, G. L. Molecular Bonding and Interactions at Aqueous Surfaces as Probed by Vibrational Sum Frequency Spectroscopy. *Chem. Rev.* **2002**, *102*, 2693−2724.

(27) Kim, G.; Gurau, M.; Kim, J.; Cremer, P. S. Investigations of Lysozyme Adsorption at the Air/Water and Quartz/Water Interfaces by Vibrational Sum Frequency Spectroscopy. *Langmuir* **2002**, *18*, 2807−2811.

(28) Jena, K. C.; Hore, D. K. Variation of Ionic Strength Reveals the Interfacial Water Structure at a Charged Mineral Surface. *J. Phys. Chem. C* **2009**, *113*, 15364−15372.

(29) van der Vegt, N. F. A.; Haldrup, K.; Roke, S.; Zheng, J.; Lund, M.; Bakker, H. J. Water-Mediated Ion Pairing: Occurrence and Relevance. *Chem. Rev.* **2016**, *116*, 7626−7641.

(30) Hess, B.; van der Vegt, N. F. A. Cation Specific Binding with Protein Surface Charges. *Proc. Natl. Acad. Sci. U. S. A.* **2009**, *106*, 13296−13300.

(31) Knackstedt, M. A.; Ninham, B. W. Correlations and Thermodynamic Coefficients in Dilute Asymmetric Electrolyte Solutions. *J. Phys. Chem.* **1996**, *100*, 1330−1335.

(32) Guldbrand, L.; Jönsson, B.; Wennerström, H.; Linse, P. Electrical Double Layer Forces. A Monte Carlo Study. *J. Chem. Phys.* **1984**, *80*, 2221.

(33) Buchner, R.; Capewell, S. G.; Hefter, G.; May, P. M. Ion-Pair and Solvent Relaxation Processes in Aqueous Na2SO4 Solutions. *J. Phys. Chem. B* **1999**, *103*, 1185−1192.

(34) Eiberweiser, A.; Buchner, R. Ion-pair or Ion-Cloud Relaxation? On the Origin of Small-Amplitude Low-Frequency Relaxations of Weakly Associating Aqueous Electrolytes. *J. Mol. Liq.* **2012**, *176*, 52−59.

(35) Wachter, W.; Kunz, W.; Buchner, R. Is There an Anionic Hofmeister Effect on Water Dynamics? Dielectric Spectroscopy of

DOI: 10.1021/jacs.9b00295
J. Am. Chem. Soc. 2019, 141, 6609−6616

Aqueous Solutions of NaBr, NaI, NaNO3, NaClO4, and NaSCN. *J. Phys. Chem. A* **2005**, *109*, 8675−8683.
(36) Santos, M. M.; Guedes de Carvalho, J. K. F.; Guedes de Carvalho, R. A. Determination of the Association Constant of NaSO4- with the Sodium-Selective Electrode. *J. Solution Chem.* **1975**, *4*, 25−29.
(37) Luts, P.; Vanhees, J. L. C.; Yperman, J. H. E.; Mullens, J. M. A.; van Poucke, L. C. Potentiometric Investigation of NaSO4- Ion Pair Formation in NaClO4 Medium. *J. Solution Chem.* **1992**, *21*, 375−382.

DOI: 10.1021/jacs.9b00295
J. Am. Chem. Soc. 2019, 141, 6609−6616